Synthesis and Optoelectronic Properties of A Novel Electrochromic Polymer through Electropolymerization of 4-(carbazol-9-yl)triphenylamine

101-2221-E-027-028-MY3

Hui-Min Wang (王惠民), Sheng-Huei Hsiao (蕭勝輝)*
Department of Chemical Engineering and Biotechnology, National Taipei University of Technology
(國立臺北科技大學化學工程與生物科技系)
E-mail: shhsiao@ntut.edu.tw

Abstract

A new carbazole and triphenylamine-containing monomer, 4-(carbazol-9-yl)triphenylamine was synthesized and coated onto ITO-glass surface by electrochemical oxidative polymerization. The elecrtrogenerated films showed two reversible oxidation redox couple on their cyclic voltammograms. The electrogenerated polymer films exhibited reversible electrochemical processes and stable color changes upon electro-oxidation, which can be switched by potential modulation. The remarkable electrochromic behavior of the film is clearly interpreted on the basis of spectroelectrochemical studies.

1. Introduction

Over the past 25 years, there has been a growing interest for conducting polymers, both polyenes and polyaromatics, such as polyaniline, polycarbazole, polythiophene, and poly(*p*-phenylene).[1] Conducting polymers can be grown electrochemically or chemically from suitable oxidizable monomers. These polymers have been found to be useful materials for sensors,[2] actuators,[3] polymeric batteries,[4] photovoltaics,[5] and electrochromic devices (ECDs).[6] ECDs based on conducting polymers can be easily and cheaply produced compared with those obtained from inorganic materials. While electrochromic polymers was mostly of academic and commercial interest, the increased solubility and conductivity of modern conductive polymers obtained by different means including electropolymerization has led to the development of ECDs.[7] They have several advantages owing to a fast response time arising from their high conductivity and easy color tuning by controlling the effective π-conjugation length.[8]

Carbazole are well-known hole-transporting and light-emitting units. Carbazole could be easily functionalized at its 3,6-, 2,7-, or *N*-positions and then covalently linked to polymeric systems, both in the main chain as building blocks and in a side chain as pending groups.[9] Polymers containing carbazole moieties in the main chain or side chain have attracted much attention because of their unique properties, which allow various optoelectronic applications such as photoconductive, electroluminescent, electrochromic, and photorefractive materials.[10] As a class of excellent electrochromic materials, triarylamine-containing high-performance polymers such as aromatic polyamides and polyimides have various useful properties such as easily forming relatively stable polarons (radical cations), high carrier mobility, high thermal stability, and good mechanical properties.[11] It has been demonstrated that *N*-substituted carbazoles can form extremely stable biscarbazoles upon anodic oxidation.[12] Therefore, various carbazole-containing electrochomic polymeric films have been prepared via the electrochemical dimerization of carbazole units.[13] However, to our best knowledge, there are still no reports about the electrosynthesis and electrochromic properties of electroactive polymers from triphenylamine-containing carbazole derivatives.

In this study, two triphenylamine-carbazole monomers (coded with **TPACz** and **MeOTPACz**, Scheme 1) are synthesized and their polymers are successfully synthesized by electrochemical oxidation of the monomers. The electrochemical and electrochromic properties of the electrogenerated films are also investigated. An ECD based on **PTPACz** from the electropolymerization of **TPACz** is also constructed and characterized. The device shows good electrochromic stability and high optical contrast ratios.

2. Monomer synthesis

The synthetic route of monomers is outlined in Scheme 1. **TPACz** and **MeOTPACz** were prepared by Ullmann reaction from *N*-(4-aminophenyl)carbazole[14] with iodobenzene and 4-iodoanisole, respectively. IR, NMR spectroscopic techniques and X-ray crystal analysis were used to confirm the structures of the obtained monomers. Figure 1 illustrates the ^{1}H NMR and ^{13}C NMR spectra of **TPACz**. These spectra are in good agreement with their proposed molecular structures. The molecular structures of **TPACz** and **MeOTPACz** were also confirmed by single-crystal X-ray analysis from the single crystal obtained by slow crystallization of an acetonitrile solution. As shown in Figure 2, **TPACz** and **MeOTPACz** display a coplanar structure of the carbazole unit and a propeller-shaped conformation of the triphenylamine core. This conformation will hinder the close packing of polymer chains and enhance the solubility of formed polymers.

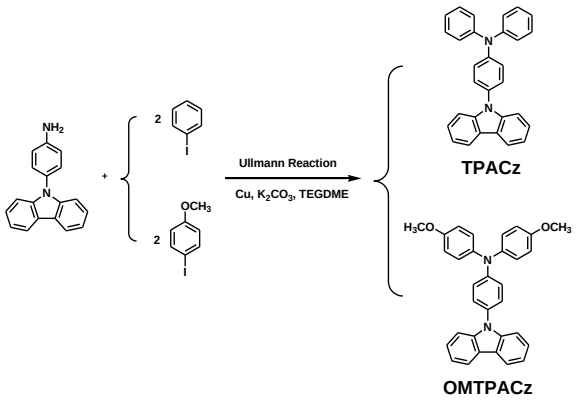

Scheme 1. Synthetic routes to monomers **TPACz** and **MeOTPACz.**

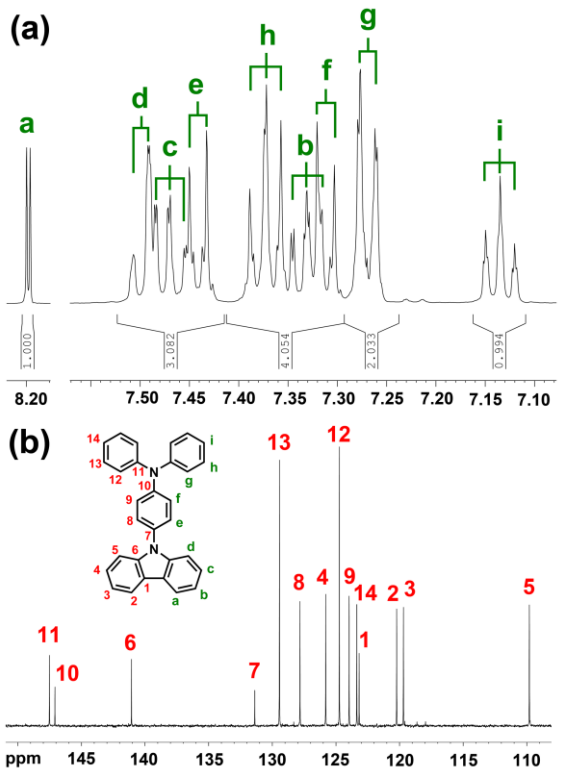

Figure 1. (a) ^{1}H NMR and (b) ^{13}C NMR spectra of **TPACz** in $CDCl_3$.

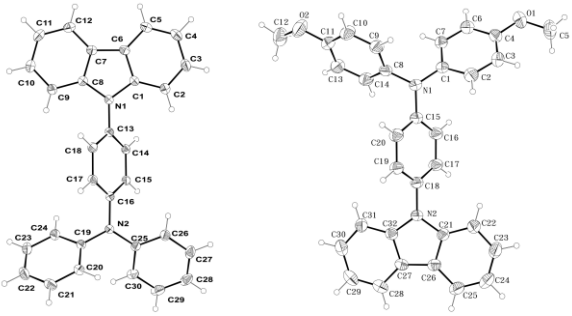

Figure 2. Molecular structures of **TPACz** and **MeOTPACz** by single crystal X-ray analysis.

3. Electrochemical polymerization

All electrochemical polymerization processes of monomers were performed on the ITO glass slides in a reaction medium containing 10^{-4} M monomer and 0.1 M Bu_4NClO_4 in acetonitrile (MeCN) via repetitive cycling at a potential scan rate of 50 mV/s. Figure 3(a) displays the successive cyclic voltammograms (CV) of the **TPACz** solution between 0 and 1.8 V. As the CV scan continued, the **PTPACz** polymer film was formed on the working electrode surface. The increase in the redox wave current densities implied that the amount of conducting polymers deposited on the electrode was increasing. The polymerization of **TPACz** showed two oxidation peaks that are attributed to their polaronic and bipolaronic states, respectively. The electrochemical properties of **MeOTPACz** are completely different [Figure 3(b)]; it displayed three oxidation couples, which indicates that the carbazole radical cations were involved in very fast electrochemical reactions that produced an **MeOTPACz** dimer [(**MeOTPACz**)$_2$] via the ring-ring coupling reaction between the carbazole units. The dimer seemed to be the major product during the oxidation process of **MeOTPACz**, due to the high stability of the oxidized states (bicarbazylium cations). No polymer films grew up on the electrode surface.

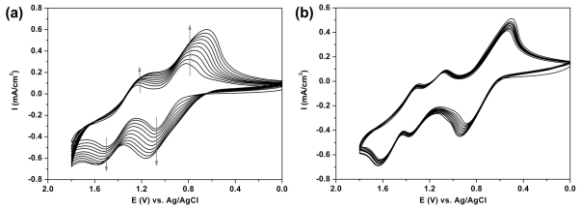

Figure 3. Repeated potential scan of (a) **TPACz** and (b) **MeOTPACz** monomers scan at rate 150 mV/s between 0 and 1.8 V in 0.1 M Bu_4NClO_4/MeCN solution.

4. Optical properties

Figure 4 shows the absorption and emission profiles of the monomers and polymers, together with their PL images on exposure to an UV light in both solution and solid states. The relevant absorption and PL data are collected in Table 1. These compounds and their derived polymers exhibited strong UV-vis absorption bands at 289-347 nm in CH_2Cl_2 solutions, assignable to the π–π* and n-π* transitions of the carbazole and triphenylamine moieties in the monomer or polymer backbone. The solid state emission spectrum was similar to that recorded from the CH_2Cl_2 solution. Although the solid-state emission of **PTPACz** was found to be slightly red shifted (ca. 13 nm) from that in solution, the emission remained in the blue region This polymer exhibited a maximum blue PL emission at 424 nm with PL quantum yield of 28.7%. The red-shift of PL maxima of polymer **PTPACz** means higher conjugation backbone in comparison with the monomer **TPACz**.

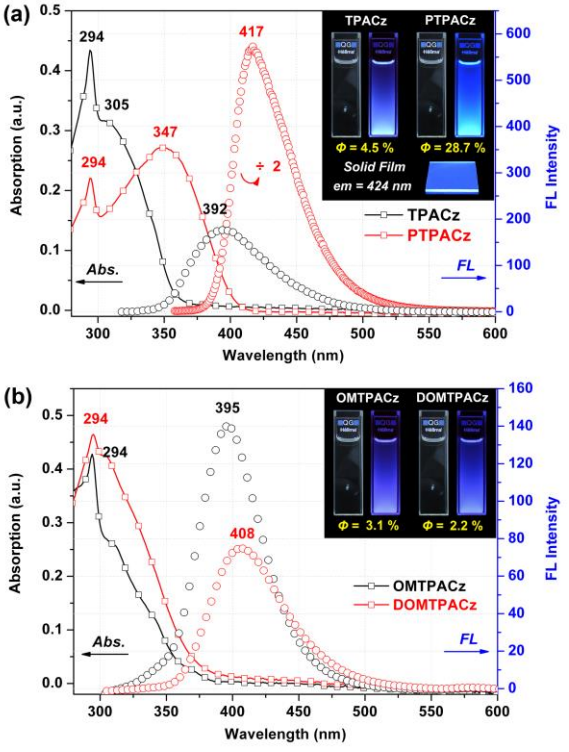

Figure 4. UV-Vis absorption and PL spectra of the dilute solutions of (a) **TPACz** and **PTPACz** (b) **MeOTPACz** and **(MeOTPACz)$_2$** in CH_2Cl_2 (1 x 10^{-5} M). Quinine sulfate dissolved in 1 M H_2SO_4 (aq.) with a concentration of 1 x 10^{-5} M as the standard (Φ_F = 54.6%). Photos show PL images of the solutions upon UV exposure (excited at 365 nm).

Table 1. Optical and Electrochemical Properties of Monomers and Polymers

Index	In Solution			As Solid Film[d]			Oxidation Potential			Energy Levels		
	λ_{max}^{abs} (nm)	λ_{max}^{PL} (nm)	Φ_{PL} (%)[c]	λ_{max}^{abs} (nm)	λ_{onset}^{abs} (nm)	λ_{max}^{PL} (nm)	$E_{1/2}^{Ox1}$ (V)	$E_{1/2}^{Ox2}$ (V)	$E_{1/2}^{Ox3}$ (V)	E_g[f] (eV)	HOMO[g] (ev)	LUMO[h] (ev)
TPACz	294, 305	392	4.5	298, 311	364	—	0.96	1.42	—	3.41	5.31	1.91
PTPACz	294, 347	417	28.7	298, 360	404	424	0.88	1.47	—	3.07	5.24	2.17
MeOTPACz	294	395	3.1	298, 310	375	—	0.71	1.30[e]	—	3.30	5.07	1.77
(MeOTPACz)$_2$	294	408	2.2	298, 310	390	—	0.71	1.20	1.46	3.18	5.07	1.89

[a] Measured in dilute solutions in CH_2Cl_2 at a concentration of about 1 x 10^{-5} mol/L. [b] Excited at the absorption maximum. [c] The fluorescent quantum yield was calculated in an integrating sphere with quinine sulfate as the standard (Φ_{PL} = 54.6%). [d] Drop-coated from CH_2Cl_2 solution. [e] Irreversible peak potential ($E_{p,a}$). [f] Optical band gap obtained from $E_g = 1240/\lambda_{edge}$. [g] The HOMO energy levels were calculated from $E_{1/2}$ and were referenced to ferrocene (4.8 eV). [h] LUMO = HOMO - E_g

The corresponding highest occupied molecular orbital (HOMO) and lowest unoccupied molecular orbital (LUMO) of **TPACz** optimized in the S_0 state could be predicted as shown in Figure 5. In the HOMO level, conjugation throughout the carbazole unit extended to the phenyl ring, despite it being twisted carbazole plane, whereas the LUMO level required the charge separation localized in carbazole core.[15]

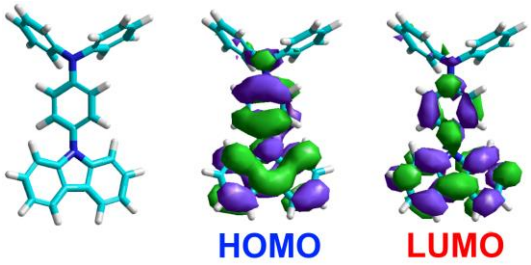

Figure 5. Optimized geometry and spatial distributions of the HOMO and LUMO levels for **TPACz**

5. Electrochemical properties

The electrochemical behavior of the electrodeposited polymer films was investigated by CV in a monomer-free Bu_4NClO_4/CH_3CN solution. The quantitative details are summarized in Table 2. The CV diagrams of monomers **TPACz** and **MeOTPACz** are shown in Figure 6. There are two reversible oxidation redox couples for **TPACz**, and one reversible redox couple and one irreversible oxidation redox wave for **MeOTPACz**, respectively. In the case of polymer **PTPACz** and dimer **(MeOTPACz)$_2$**, as shown in the Figure 7, the CV of **PTPACz** reveal two reversible oxidation redox couples at half-wave potentials ($E_{1/2}$) of 0.88 V and 1.47 V. The first electron removal for **PTPACz** is assumed to occur at the triphenylamine segment, which is more easily oxidized than the carbazole moiety. The HOMO (highest occupied molecular orbital) energy levels of the investigated polyamides were calculated from the half-wave potentials of the first oxidation wave ($E_{1/2}^{ox1}$) and by comparison with ferrocene (4.8 eV). These data together with absorption spectra were then used to obtain the LUMO (lowest unoccupied molecular orbital) energy levels (Table 1). According to the HOMO and LUMO energy levels obtained, the polyamide in this study appear to be appropriate as hole injection and transport materials.

6. Spectroelectrochemical properties

Spectroelectrochemistry were performed on the electrogenerated polymeric films on ITO glass to clarify its electronic structure and optical behavior upon oxidation.

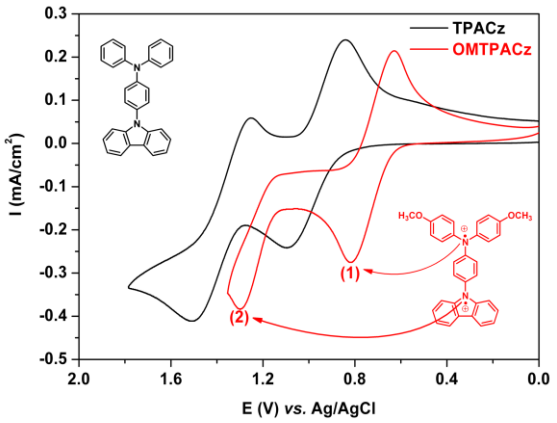

Figure 6. Cyclic voltammograms of **TPACz** and **MeOTPACz** monomers in 0.1 M Bu_4NClO_4/CH_3CN solution at scan rate 50 mV/s.

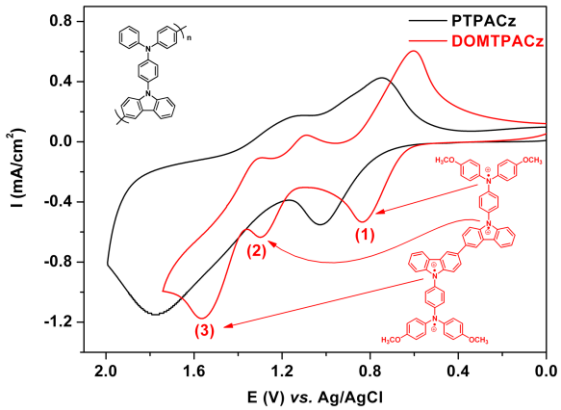

Figure 7. Cyclic voltammogram of **PTPACz** and the **(MeOTPACz)$_2$** dimer in 0.1 M Bu_4NClO_4/CH_3CN solution at scan rate 50 mV/s.

The typical UV-vis-NIR absorption spectra and electrochromic behavior of **PTPACz** at various applied potentials are illustrated in Figure 8. In the neutral form, at 0 V, **PTPACz** exhibited strong absorption at wavelength around 306 nm, characteristic for π-π* transitions, but it was almost transparent in the visible and near infrared (NIR) regions. The band gap of polymer **PTPACz** was calculated as 3.41 eV from the onset of the π-π* transition. Upon oxidation of the **PTPACz** film (increasing applied voltage from 0 to 1.00 V), the intensity of the absorption peak at 414 nm and a broadband from 800 nm extended to 1100 nm in the NIR region grew up. Since the potentials examined are similar to the first anodic process, the spectral changes are assigned to the radical cation (polaron)

formation arising from the oxidation of TPA unit. The absorption band in the NIR region may be attributed to an intervalence charge transfer (IVCT) between states in which the positive charge is centered at different amino centers (TPA and carbazole). The IVCT phenomenon of the family of triarylamines has been reported in literature.[16] Upon further oxidation at applied voltages to 1.8 V, the dication (bipolaron) band at 727 nm formed. Concurrently, the IVCT band and the absorption peak at 414 nm decreased in intensity during this process. The observed electronic absorption changes in the film of **PTPACz** at various potentials are fully reversible and are associated with strong color changes; indeed, they even can be seen readily by the naked eye. As shown in Figure 8 inset, it can be seen that the film of **PTPACz** switches from a transmissive neutral state (nearly colorless) to a highly absorbing semi-oxidized state (orange or green) and a fully oxidized state (blue).

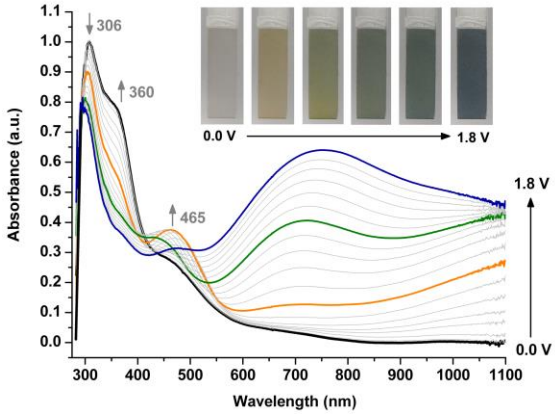

Figure 8. Spectroelectrochemical spectra of **PTPACz** with applied potential between 0 and 1.8 V in Bu_4NClO_4/CH_3CN solution.

7. Electrochromic Devices

Finally, we fabricated as preliminary investigations single layer electrochromic cells (Figure 9). The polymer films were electrodeposited onto ITO-coated glass, thoroughly rinsed, and then dried. Afterwards, the gel electrolyte was spread on the polymer-coated side of the electrode and the electrodes were sandwiched. To prevent leakage, an epoxy resin was applied to seal the device. As a typical example, an electrochromic cell based on **PTPACz** was fabricated. When the voltage was applied (from 0.0 to 1.8 V, 2.0 V and 2.4 V, respectively), the color changed yellow, green, and deep blue, respectively, the same as those were already observed in the spectroelectrochemical experiments. When the potential was subsequently set back at 0.0 V, the polymer film turned back to original color. We believe that optimization could further improve the device performance and fully explore the potential of these electrochromic polymers.

8. Conclusions

A new electrochromic polymer have been readily prepared from 4-(carbazol-9-yl)triphenylamine by electrochemical oxidative polymerization. The polymer film revealed excellent electrochemical and electrochromic stability with multielectrochromic behavior. The solid ECD presented a stable as well as multicolor electrochromic change from colorless to yellow or green and then to dark blue. Its environmental friendliness, easy preparation, abundant color, fairly fast electrochromic switching at low voltages, along with their stability under atmospheric conditions, made the ECD good candidates for electrochromic display.

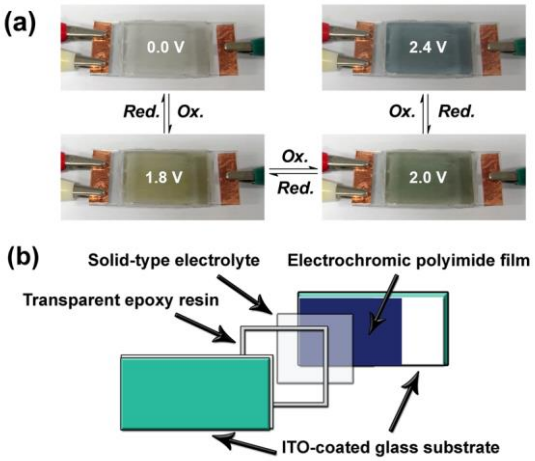

Figure 9. (a) Photos of sandwich-type ITO-coated plastic single layer electrochromic device, using **PTPACz** as active layer. (b) Schematic illustration of the structure of the ECD.

References

1. Groenendaal, L.; Jonas, F.; Freitag, D.; Pielartzik, H.; Reynolds, J. R. *Adv. Mater.* **2000**, *12*, 481.
2. Josowicz, M.; Janata, J. *Anal. Chem.* **1986**, *58*, 514.
3. Pei, Q.; Jarvinen, H.; Osterholm, J. E.; Ingana¨ s, O.; Laakso, J. *Macromolecules* **1992**, *25*, 4297.
4. Gofer, Y.; Sarker, H.; Killian, J. G.; Poehler, T. O.; Searson, P. C. *Appl. Phys. Lett.* **1997**, *71*, 1582.
5. Yohannes, T.; Inganas, O. *J. Electrochem. Soc.* **1996**, 143, 2310.
6. Garnier, F.; Tourillon, G.; Gazard, M.; Dubois, J. C. *J. Electrochem. Soc.* **1983**, *148*, 299.
7. (a) Tran-Van, F.; Beouch, L.; Vidal, F.; Yammine, P.; Teyssi'e, D.; Chevrot, C. *Electrochim. Acta* **2008**, *53*, 4336; (b) Rosseinsky, D. R.; Mortimer, R. J. *Adv. Mater.* **2001**, *13*, 783.
8. Beaujuge, P.M.; Reynolds, J. R. *Chem. Rev.* **2010**, *110*, 268.
9. (a) Chen, J. P.; Natansohn, A. *Macromolecules* **1999**, *32*, 3171; (b) Morin, J.-F.; Leclerc, M.; Ades, D.; Siove, A. *Macromol. Rapid Commun.* **2005**, *26*, 761.
10. Boudreault, P.-L.; T., Beaupre, S.; Leclerc, M. *Polym. Chem.* **2010**, *1*, 127.
11. Yen, H.-J.; Liou, G.-S. *Polym. Chem.* **2012**, *3*, 255.
12. Ambrose, J. F.; Nelson, R. F. *J. Electrochem. Soc.* **1968**, *115*, 1159.
13. (a) Natera, J.; Otero L.; D'Eramo, F.; Sereno, L.; Fungo, F.; Wang, N.-S.; Tsai, Y.-M.; Wong, K.-T. *Macromolecules* **2009**, *42*, 626; (b) Xu, C.; Zhao, J.; Wang, M.; Wang, Z.; Cui, C.; Kong, Y.; Zhang, X. *Electrochim. Acta* **2012**, *75*, 28-34.
14. Liou, G.-S.; Hsiao S.-H.; Chen H.-W. *J. Mater. Chem.* **2006**, *16*, 1831.
15. Wang, T.-T.; Chung, S-M.; Wu, F.-I.; Shu, C.-F.; Diau, E. W.-G. *J. Phys. Chem. B* **2005**, *109*, 23827.
16. Lambert, C.; Noll, G. *J. Am. Chem. Soc.* **1999**, *121*, 8434.